CHANNELS
2024, VOL. 18, NO. 1, 2294661
https://doi.org/10.1080/19336950.2023.2294661

Taylor & Francis
Taylor & Francis Group

RESEARCH ARTICLE

OPEN ACCESS Check for updates

A phenylalanine at the extracellular side of Kir1.1 facilitates potassium permeation

Henry Sackin and Mikheil Nanazashvili

Department of Physiology and Biophysics and Center for Proteomics and Molecular Therapeutics, Chicago Medical School, Rosalind Franklin University, North Chicago, IL, USA

ABSTRACT

The Kir1.1 (ROMK) family of weak inward rectifiers controls K secretion in the renal CCT and K recycling in the renal TALH. A single point mutant of the inward rectifier, F127V-Kir1.1b was used to investigate the K transition between the selectivity filter and the outer mouth of the channel. We hypothesize that normally an aromatic *Phe* at the external entryway of Kir1.1b facilitates outward K secretion. We tested this by replacing F127-Kir1.1b with a small aliphatic *Val*. Results indicate that removal of the *Phe* at 127 suppresses outward currents that normally contribute to K secretion. Results with the F127V mutant could be explained by increased polyamine block and/or a decrease in the avidity of Kir1.1 for K ions near the outer mouth of the channel. The latter is supported by F127V-Kir1.1b having a lower affinity (K_m = 33 mM) for K than wild-type Kir1.1b (K_m = 7 mM) during external K elevation. Conversely, chelation of K with 18-Crown-6 ether reduced K conductance faster in F127V (half-time = 6s) than in wt-Kir1.1b (half-time = 120s), implying that F127V is less hospitable to external K. In other experiments, positive membrane potentials gated the F127V mutant channel closed at physiological levels of external Ca, possibly by electrostatically depleting K adjacent to the membrane, suggesting that the *Phe* residue is critical for outward K secretion at physiological Ca. We speculate that the avidity of wt-Kir1.1b for external K could result from a cation-Pi interaction between K and the aromatic F127.

ARTICLE HISTORY
Received 1 September 2023
Revised 27 November 2023
Accepted 8 December 2023

KEYWORDS
Inward rectifier; ROMK; channel; selectivity filter; renal; regulation

Introduction

Crystallographic and cryo-EM studies on members of the inward rectifier family have characterized many structural aspects of Kir2 [1,2], Kir3 [3] and Kir 6 [4]. In addition, a vast number of physiological experiments have provided indirect information about inward rectifier structure and function. These have been summarized extensively in a variety of review articles. However, the Kir1.1 family of weak inward rectifiers, that play an important role in renal K secretion in the collecting tubule and K recycling in the thick ascending limb, remain poorly characterized at the atomic level with little detail about K exit and entry between free solution and selectivity filter.

One particular *Phe* residue (F127-Kir1.1b) at the extracellular side of all 4 identical Kir1.1 subunits is adjacent to the GYG selectivity sequence and is conserved throughout the human and rat Kir1.1 family. It is also conserved in the strong inward rectifier Kir2.1 and in Kir3.4 and Kir4.1 (Figure 1). However an aromatic *Tyr* occurs at this position in Kir3.1, Kir3.2, and Kir5.1. From an evolutionary standpoint, this suggests that interaction between K and an aromatic residue at the equivalent of 127-Kir1.1b might be important for the physiologic function of these inward rectifiers. Furthermore, additional aromatics at loci corresponding to 129-Kir1.1b (Phe in Kir1.1b and Tyr in Kir3.1, Kir4.1) raise the possibility that one, or both, of the aromatic residues form cation–Pi interactions with K ions just exterior to the selectivity filter. Even in other channel families (Kv, KcsA, and KirBac), the residue corresponding to 127-Kir1.1b is a negatively charged acidic *Asp* residue which might also attract external K to the outer mouth of the pore.

The underlying hypothesis of the present study is that the aromatic *Phe* at F127-Kir1.1b interacts with fully hydrated extracellular K ions, allowing

CONTACT Henry Sackin henry.sackin@rosalindfranklin.edu

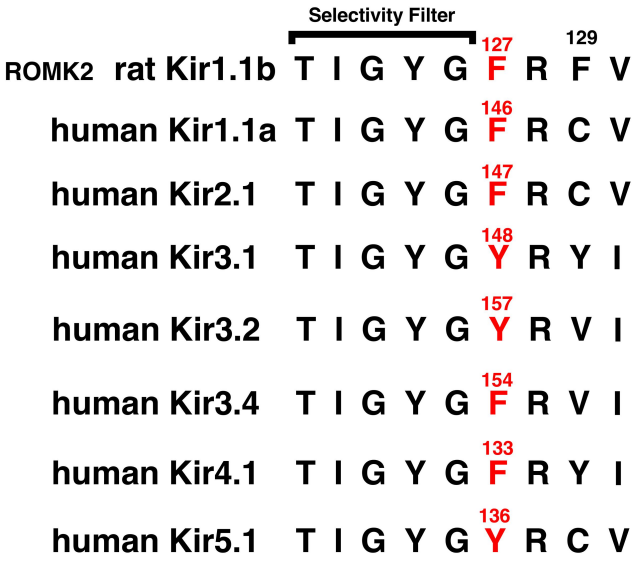

Figure 1. Comparison of inward rectifier K channel sequences near the TIGYG selectivity filter, indicating the presence of either a *Phe* or a *Tyr* aromatic residue just outside the selectivity filter.

K to more readily adopt a partially hydrated S0 state, prior to entering the selectivity filter in a fully dehydrated state [5]. In this manner, F127-Kir1.1b facilitates the entry and exit of K into and out of the channel to optimize K secretion in the renal collecting tubule and K recycling in the renal thick ascending limb. We tested this hypothesis by replacing the *Phe* at 127-Kir1.1b with a small aliphatic *Val* and examining its effect on both single-channel and whole-cell conductance. Of particular interest was the effect of F127V-Kir1.1b on macroscopic outward K currents.

Materials and methods

Mutant construction and expression of channels

We engineered point mutations in Kir1.1b (ROMK2; EMBL/GenBank/DDBJ accession No. L29403) using a polymerase chain reaction QuickChange mutagenesis kit (Stratagene) and primers synthesized by Integrated Data Technologies (Coralville, IA). Nucleotide sequences were checked on an Applied Biosystems 3100 DNA sequencing machine at the University of Chicago Cancer Research Center.

Plasmids were linearized with Not I restriction enzyme and transcribed in vitro with T7RNApolymerase in the presence of the GpppG cap by means of an mMESSAGEmMACHINEkit (Ambion, Austin, TX). Synthetic cRNA was dissolved in water and stored at 70°C before use. Stage V-VI defolliculated Xenopus oocytes were obtained directly from Ecocyte Bio Science (Austin TX). Oocytes were injected with 5–10 ng of cRNA, and incubated at 19°C in 2× diluted Leibovitz medium (Life Technologies, Grand Island, NY) for 1–3 days before measurements were made.

Whole-cell experiments

Whole-cell conductances measured with the two-electrode voltage clamp provide a simple measure of aggregate channel activity. We measured whole-cell currents and conductances in intact oocytes using a two-electrode voltage clamp (model CA-1; Dagan, Minneapolis, MN) with 16 command pulses of 20 ms duration between −160 mV and +100 mV, centered around the resting potential. Oocytes expressing Kir1.1b or the mutant F127V-Kir1.1b were bathed in permeant acetate buffers to control their internal pH as previously described, where the relation between intracellular (i) and extracellular (o) pH is given by:

$pHi = 0.595 \times pHo + 2.4$ [6]. In the present study, the bath was acetate buffered to pHo = 8.4 to produce an internal oocyte pHi of 7.4, which was sufficient to maintain the primary channel gate at the bundle crossing in an open conformation [7]. There was no external pH dependence of single-channel conductance or gating for the channels used in this study, as determined in separate experiments with impermeant external buffers.

The bath for the whole-cell experiments consisted of 50mMKCl, 50 mM K acetate, ±2 mM $CaCl_2$, and 5 mM HEPES. In low-K solutions, NaCl and NaAcetate replaced KCl and KAcetate, respectively, where all solutions had the same ionic strength. The 0 Ca, 0 Mg solutions contained 1 mM EGTA. The zero K external solutions had no added K and contained 15 mM of the K chelator 18-Crown-6 (crown ether, catalog No. 274984, Sigma-Aldrich). A fast flow chamber perfusion system was used to exchange 95% of the bath volume of 0.5 ml in 2s. The time course of the bath exchange was determined from the change in whole oocyte reversal potential during exposure

to different external K solutions. Complete whole-cell current-voltage curves for both wild-type and the F127V mutant were automatically generated in 320 ms (16 pulses@20 ms) for each of the experimental conditions. This is significantly faster than the 2s required to exchange the bath, which avoids any perfusion-dependent ambiguities in the conductance measurements.

Much of the whole-cell I-V data are presented as representative experiments showing wild-type or mutant currents resulting from different external K concentrations applied to the same oocyte. This permitted each oocyte to effectively function as its own control and avoided the problem of variable channel expression that plagues whole-oocyte experiments. In some cases normalized I-V data were used. Finally, oocytes were checked for endogenous chloride currents, and oocytes exhibiting chloride conductances >2 μS were not used.

Single-channel methods

The oocytes reserved for single-channel measurements were subjected to a hypertonic shrinking solution, thereby allowing easy removal of the vitelline membrane, prior to patching. Pipettes were pulled from Warner Patch glass (G85165T–3) on a two-stage puller (HEKA, PIP5), coated with Sylgard prior to use, and filled with the indicated KCl concentration, plus the appropriate NaCl to achieve 100 mM, and buffered with 10 mM HEPES. For the Ca experiments, Ca was added to the pipette solution as indicated in the protocol. Patch currents were recorded with a Dagan 8900 patch-clamp amplifier, visualized on an Atari-based acquisition system and stored, unfiltered, on videotape. For analysis, current records were replayed from videotape, sampled at 5 kHz, low-pass filtered at 900 Hz, and analyzed using MacTAC software (superseded by HEKA Patchmaster), run on a Mac operating system.

Homology models of Kir1.1b and the mutant F127V-Kir1.1b were generated using MOE (Molecular Operating Environment, Montreal, Canada) with the closed-state 3.1 angstrom crystal structure of the chicken inward rectifier Kir2.2 (3JYC) as template.

Results

The F127V single point mutation profoundly altered the electrical characteristics of Kir1.1b, the rat outer medullary K channel (ROMK2), that belongs to the family of weak inward rectifiers whose physiological importance derives from secreting outward K (from cell to lumen), despite having a higher conductance in the inward direction.

Wild-type Kir1.1b single channels

Figure 2a illustrates single channel current from wt-Kir1.1b, together with its associated current-voltage (I-V) relation (Figure 2b). Oocytes were depolarized to near zero membrane potential by 100 mM K in the bath since oocyte average internal [K] was close to 100 mM. Hence, the membrane patch potential is the negative of the pipette command potential. Although the bath contained 2 mM Ca and 1 mM Mg to maintain oocyte viability, bath Ca and Mg never entered the pipette because slight positive pressure was always applied prior to patching.

As indicated in Figure 2b, native Kir1.1b channels conduct current much better in the inward direction with a typical inward single-channel conductance of 25pS, for this representative experiment (thin-dashed line, Figure 2b). At positive voltages the outward current progressively falls off, indicative of internal polyamine and Mg block. Nonetheless, outward current in wild type Kir1.1b is still sufficient to contribute to renal K secretion in cortical collecting tubule and K recycling in thick ascending limb.

F127V mutation suppresses outward K current

The F127V-Kir1.1b mutant differs from wt-Kir1.1b most notably by its strong rectification and marked suppression of outward K current at large (inside positive) potentials, as well as a negative slope conductance at V > +50 mV (Figure 3). This suppression of current at positive potentials is uncharacteristic of Kir1.1 weak inward rectifiers but is seen with strong inward rectifiers, Kir2 [8,9] and Kir6.2 [10]. Data for Figure 3 were obtained from F127V single channel

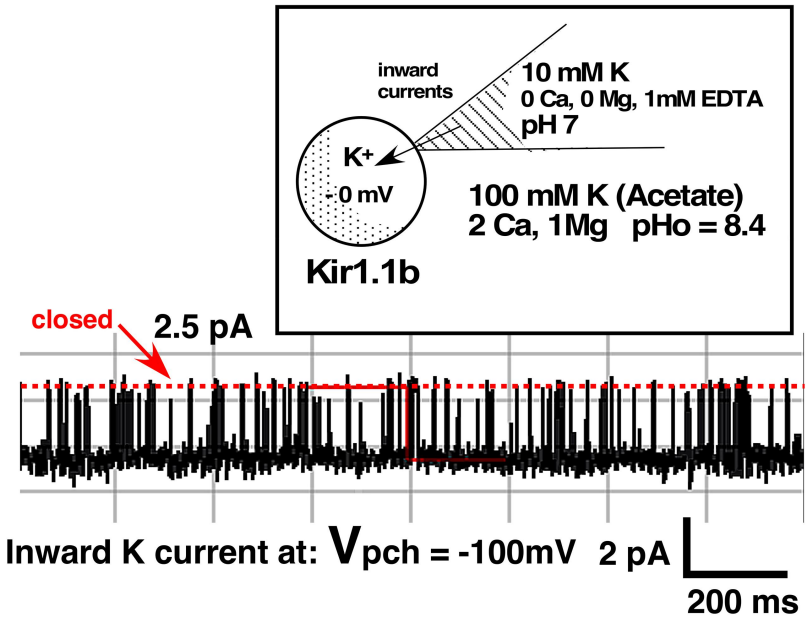

Figure 2a. Representative Kir1.1b single channel inward current record in a cell-attached patch with 10 mM K, zero Ca in the pipette (outside of channel). Oocytes were depolarized by 100 mM K in the bath, which maintained internal oocyte [K] near 100 mM and allowed the patch potential to be calculated as the negative of the pipette command potential. Inward current averaged 2.5 pA at a patch voltage of −100 mV (inside negative). In this and all subsequent figures, permeant acetate buffers at pHo = 8.4 maintained internal oocyte pHi = 7.4, which guarantees that the Kir1.1 bundle crossing gate remains open.

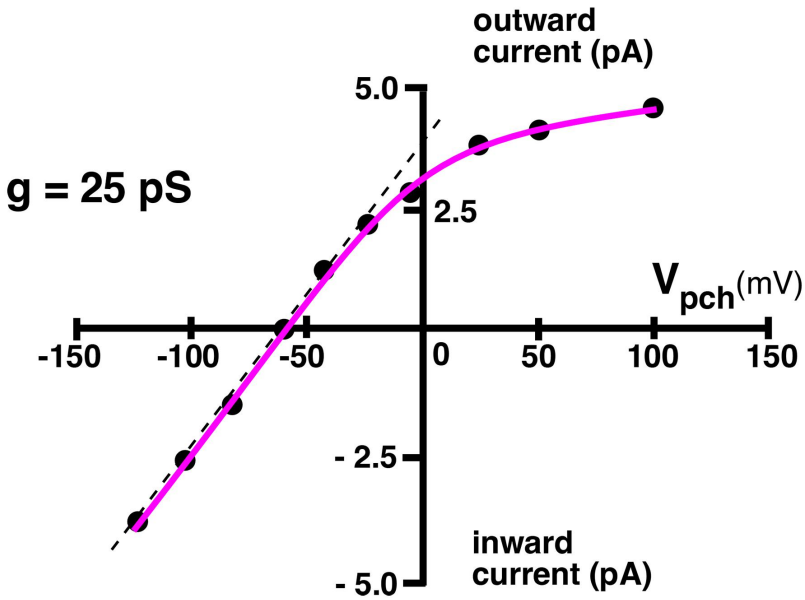

Figure 2b. The single channel current voltage relation corresponding to the cell-attached patch of Figure 2a with 10 mM pipette K (outside surface) and a presumed internal [K] of 100 mM in this 100 mM external K depolarized oocyte. Single channel inward conductance was 25 pS (dashed line) and the reversal potential was −59 mV in this recording, indicating a high K selectivity for a 10 fold K ratio across the patch.

recordings in 5 patches on 5 separate oocytes. Solid circles represent average currents ± SE at each patch voltage.

Although inward rectification in the Kir family is largely attributable to internal block by Mg and polyamines [11], the residues responsible for this

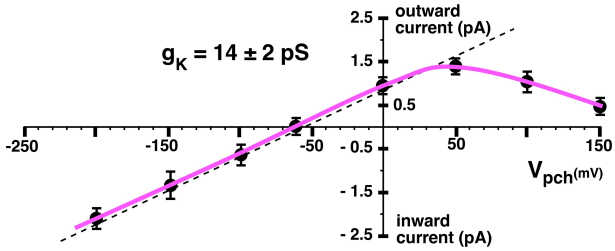

Figure 3. F127V single channel current-voltage curve for cell-attached patch recordings similar to fig 4A. The pipette contained 10 mM K, 0 Ca. Oocytes with a nominal internal [K] of 100 mM were depolarized to near zero potential by 100 mM K in the bath. Average single channel conductance (g_K) = 14 ± 2pS (n = 5 oocytes) for inward currents (dashed line), and E_{rev} = −60 mV for a 10 fold inside/outside K gradient.

block are located along the transmembrane region of the Kir2 vestibule [10]. However, if the F127V mutation decreased the channel's affinity for external K, this would decrease K in the selectivity filter, allowing increased block by internal polyamines, The net effect would be to shift the weakly rectifying Kir1.1 toward stronger rectification, analogous to Kir2.1.

In contrast to outward currents, inward F127V currents (Figure 4a) were qualitatively similar to wt-Kir1.1b (Figure 2a) but had a reduced single-channel conductance of g_K = 14 ± 2pS (n = 5 oocytes) compared to 28 ± 4pS (n = 6 oocytes) pS for wt-Kir1.1b under similar conditions (green curve, Figure 5). Reversal potentials for both F127V and Kir1.1b were approximately −60 mV, consistent with a high K selectivity for both wild-type and mutant, given the 10-fold K ratio between external (pipette) and internal (oocyte) K concentrations.

Both F127V and wt-Kir1.1 also exhibited similar inward single channel kinetics (Figure 4A,B vs Figure 2A). With 10 mM K and zero Ca in the pipette, F127V open and closed times were 19.4 ms and 3.3 ms, respectively in cell attached patches at −100 mV (Figure 4B). This is close to the average open and closed times of 20.6 ± 0.3 ms and 1.6 ± 0.2 ms (n = 5) previously reported for wt-Kir1.1b under similar conditions [7].

K-dependence of F127V single-channel conductance

The F127V mutation reduced single-channel conductance at all concentrations of pipette K (Figure 5). Steady state inward conductances were determined between −20 mV and −200 mV using cell-attached patches from oocytes bathed in different external K concentrations without Ca or Mg.

Both F127V (n = 5 patches) and wt-Kir1.1b (n = 6 patches) inward conductances were saturable functions of external (pipette) K. The data were fit with a Michaelis–Menten model to yield both maximal conductance (g_{max}) and K rate constant (K_m), where K_m represents the K concentration corresponding to half maximal inward single channel conductance (Figure 5). The F127V mutant had a K_m of 33 ± 4 mM and a maximum conductance (g_{max}) of 40 ± 2 pS (n = 5), while Kir1.1b had a K_m of 7.7 ± 1 mM and a g_{max} of 51 ± 1 pS (n = 6) (Figure 5). These conductance data are consistent with F127V having a decreased affinity for partially hydrated K ions adjacent to the outer mouth of the channel, which could alter the distribution of K in the selectivity filter and reduce conductance.

Whole-cell F127V currents and K-dependence

The difference between F127V and wt-Kir1.1b was further examined by measuring whole-cell currents using a two-electrode oocyte voltage clamp (TEVC). With 10 mM K and 0 Ca in the bath, F127V and wt-Kir1.1b had qualitatively similar macroscopic inward currents and similar reversal potentials of −59 mV for a 10-fold (in/out) K ratio, indicating a high K selectivity (Figure 6). The data of Figure 6 were normalized to maximum inward current to facilitate comparison between F127V and wt-Kir1.1b which generally have different expression levels in

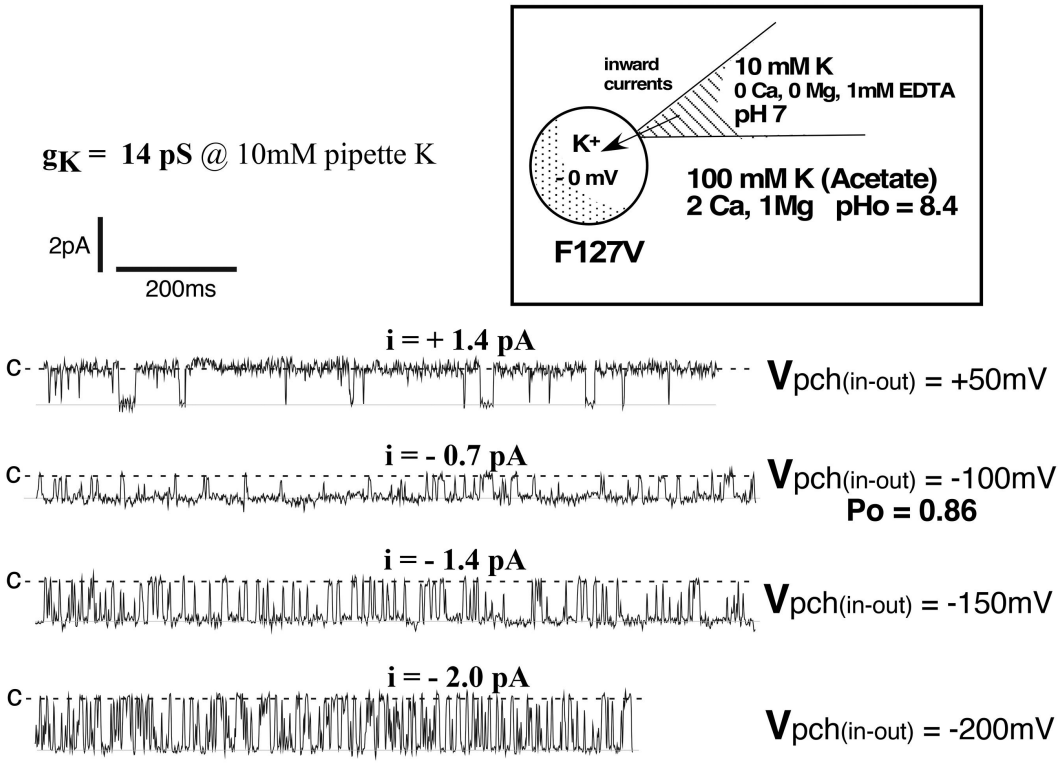

Figure 4a. Representative F127V single-channel currents for a cell-attached patch with 10 mM K and zero Ca in the pipette, similar to those used to construct the current voltage relation of Figure 3. Oocytes with a nominal internal [K] of 100 mM were depolarized to near zero potential by 100 mM K in the bath. Patch potential is indicated at the right of each tracing and the closed state is denoted by c.

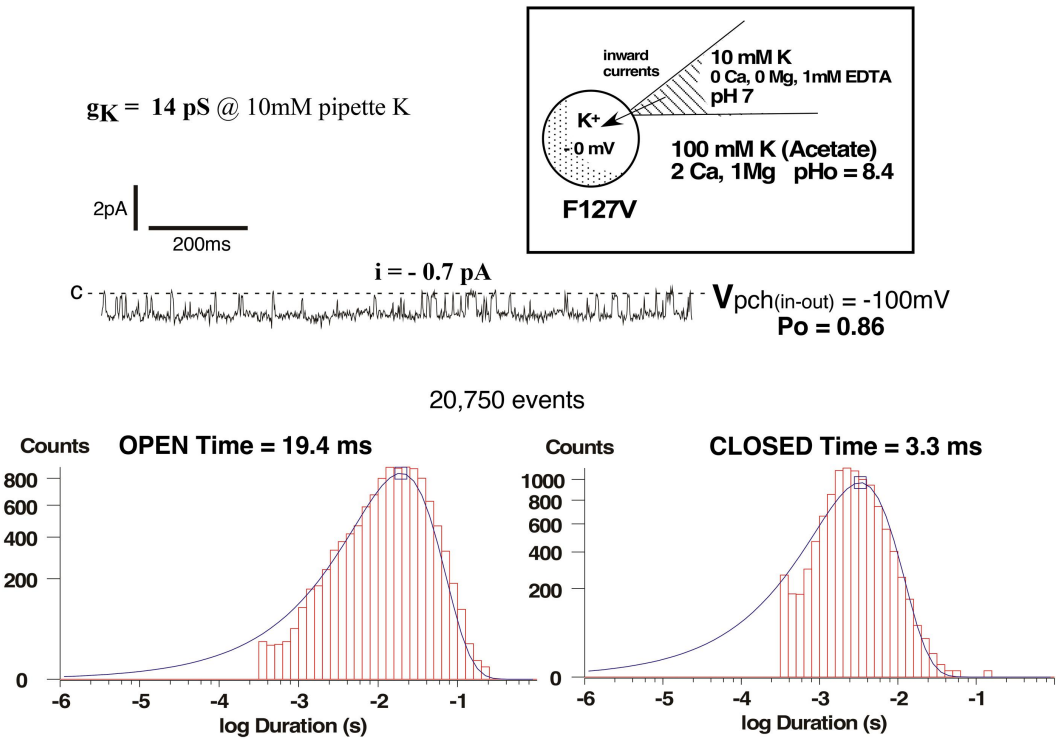

Figure 4b. Kinetics for the single-channel F127V currents of Figure 4a at a patch potential of –100 mV (inside negative). In the absence of pipette Ca, F127V is characterized by a single open time of 19.4 ms and a single closed time of 3.3 ms.

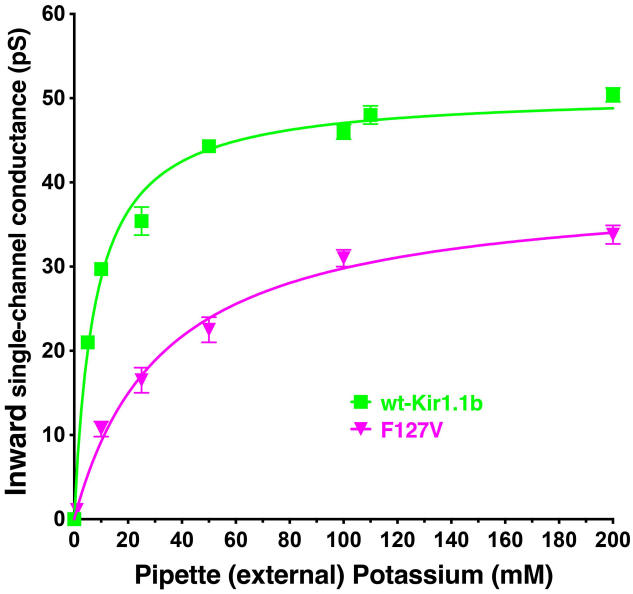

Figure 5. F127V has a lower single channel inward conductance than wild-type Kir1.1b at all external K concentrations. Data were obtained under steady state conditions in cell-attached patches at different pipette K concentrations without Ca or Mg. Oocytes were K-depolarized by 100 mM bath [K], and inward conductances were computed from linear fits of the i-v data acquired between −20 mV and −200 mV.

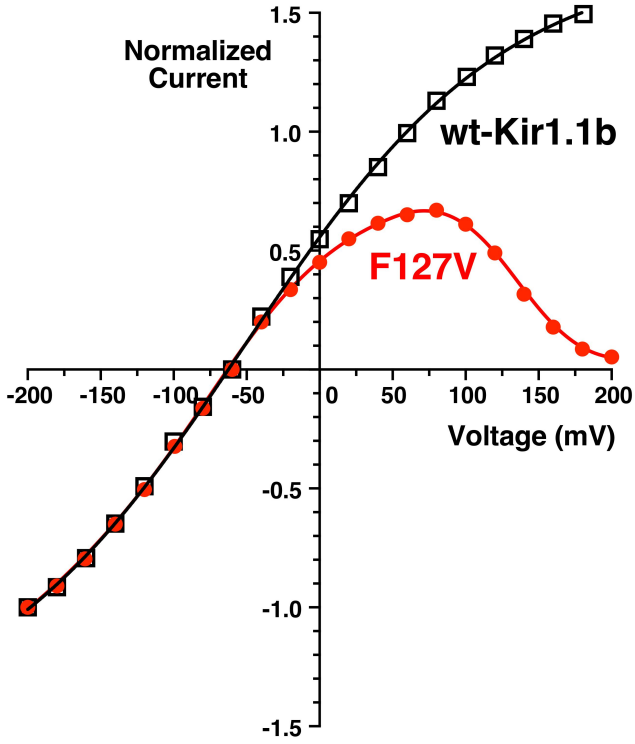

Figure 6. Positive membrane voltage suppresses whole-cell F127V outward currents (red) relative to wt-Kir1.1b (black) in a typical current-voltage relation. Data were normalized to maximum inward current to compensate for different expression levels of F127V and wt-Kir1.1b in oocytes. External bath: 10 mM K, zero Ca at pHo = 8.4 with acetate buffer. Internal oocyte [K] was not directly measured but was presumed close to its average nominal value of 100 mM. Other paired oocyte experiments yielded F127V and wt-Kir1.1b currents similar to Figure 6.

oocytes. Even though multiple experiments showed slight variations in these profiles they were all qualitatively similar to Figure 6.

Although F127V and wt-Kir1.1b inward currents were similar, their outward macroscopic currents were markedly different (Figure 6). Wild-type Kir1.1b exhibits the canonical weak rectification that characterizes the Kir1 family. However, F127V outward current was strongly suppressed by positive membrane potentials above 80 mV (red curve, Figure 6). This decline is partially the result of a similar decline in F127V single-channel current at positive voltage (Figure 3).

Relief of rectification by external K

We believe that the voltage-dependent reduction in F127V outward current at positive voltage (>80 mV) does not result exclusively from polyamine block [8]. To assess this we compared the effect of elevating external K on wt-Kir1.1b and F127V conductance curves. Figures 7 and 8 depict the results of successive K elevations on either a single Kir1.1b or a single F127V oocyte. This allowed each oocyte to effectively function as its own control. Smooth curves drawn through the data of Figures 7 & 8 have no intrinsic meaning. Other Kir1.1b oocytes ($n = 4$) and F127V oocytes ($n = 6$), examined on different days, showed similar K dependence of I-V curves, but with different absolute current levels.

We first confirmed that the elevation of external K increased both inward and outward wt-Kir1.1b conductance despite a decreased driving force for outward K current (Figure 7). This increase in outward current during elevation of external K is consistent with a "relief of rectification" that had been proposed for Kir2.1 to explain the effect of external K on polyamine block [8].

Raising external K also increased F127V outward current and decreased rectification between 0 and 50 mV, similar to wt-Kir1.1b (Figures 7,8). However, external K acts differently on F127V than wt-Kir1.1b because relief of rectification

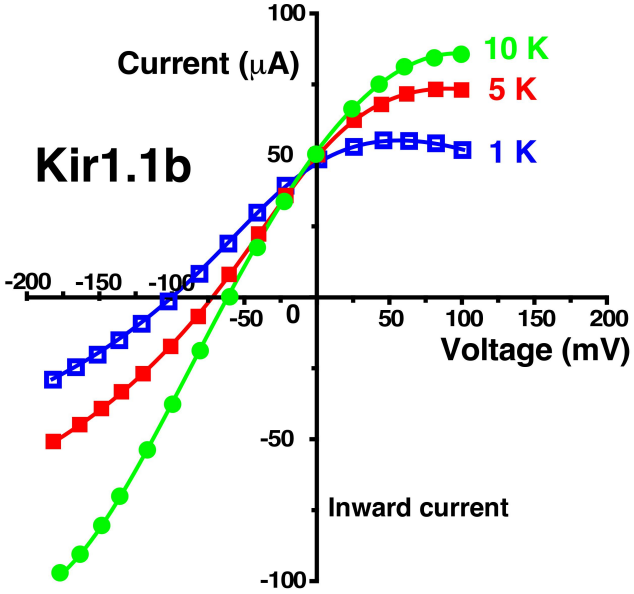

Figure 7. Relief of rectification in wt-Kir1.1b by external K elevation. Representative whole-cell current-voltage curves were obtained from an individual oocyte bathed in zero Ca, zero Mg and successive external K concentrations of 1 mM, 5 mM and 10 mM. Other oocytes ($n = 4$, obtained on different days) showed similar K dependence of their I-V curves, but with different absolute current levels. Abscissa is oocyte membrane potential relative to bath (ground). Internal oocyte [K] was not directly measured but was presumed close to it's average nominal value of 100 mM. Shifts in reversal potentials at different external K are consistent with wt-Kir1.1b having a high K selectivity.

with F127V was not sustained at positive voltages above 80 mV (Figure 8).

In addition, decreasing external K from 10 mM to 1 mM reduced both F127V inward and outward conductance much more than for wt-Kir1.1b (Figures 7,8). For example, at zero membrane potential (along the Y axis) F127V outward current declined by 3-fold upon going from 10 mM to 1 mM K (Figure 8); whereas the same decrease in external K produced no change in outward wt-Kir1.1b current at zero voltage. Hence, the F127V mutation greatly increases the sensitivity of channel current and conductance to K removal.

F127V responds faster than wild-type to external K removal

The sensitivity of F127V to external K was further explored by examining the time course of the whole-cell conductance decrease during K removal with 15 mM of the K chelator: 18-Crown-6 (catalog No. 274984, Sigma-Aldrich). The switch from 10 mM K to a zero K bath plus chelator caused a rapid (2s) decrease in both inward and outward F127V macroscopic conductance as well as a shift in reversal potential (Figure 9). Complete I-V curves at 10 mM and zero mM external K could be generated within 320msec (16 pulses of 20 ms), which was significantly less than the time of 2s needed for a 95% bath exchange.

Average data from F127V ($n = 5$) and Kir1.1b ($n = 6$) oocytes, similar to Figure 9, are summarized in Figure 10 and fit to standard exponential decay models of the form: $(G\text{-}G_{\infty})\exp(-k\bullet t) + G_{\infty}$, where Ln(2)/k equals the half-time of the conductance decline. Subjecting wt-Kir1.1b to similar transitions

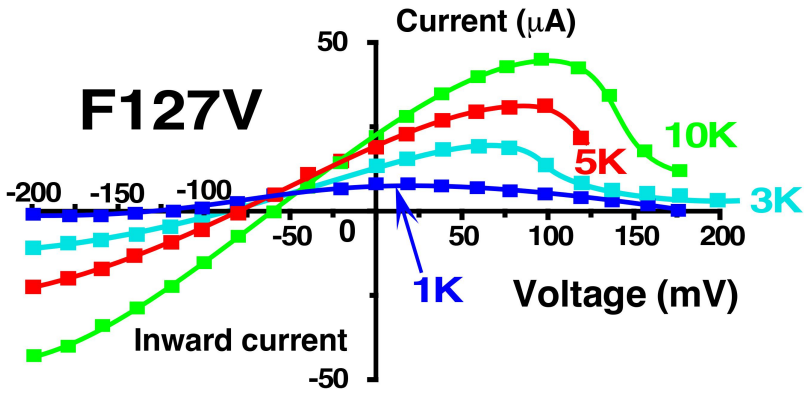

Figure 8. Effect of external K on the whole cell **F127V-Kir1.1b** current-voltage relation. Representative whole-cell current-voltage curves were obtained from an individual oocyte bathed in zero Ca, zero Mg and successive external K concentrations between 1 mM and 10 mM. Other oocytes ($n = 6$, obtained on different days) showed similar K dependence of their I-V curves, but with different absolute current levels. Abscissa is oocyte membrane potential relative to bath (ground). Shifts in reversal potentials at different external K are consistent with F127V-Kir1.1b having a high K selectivity.

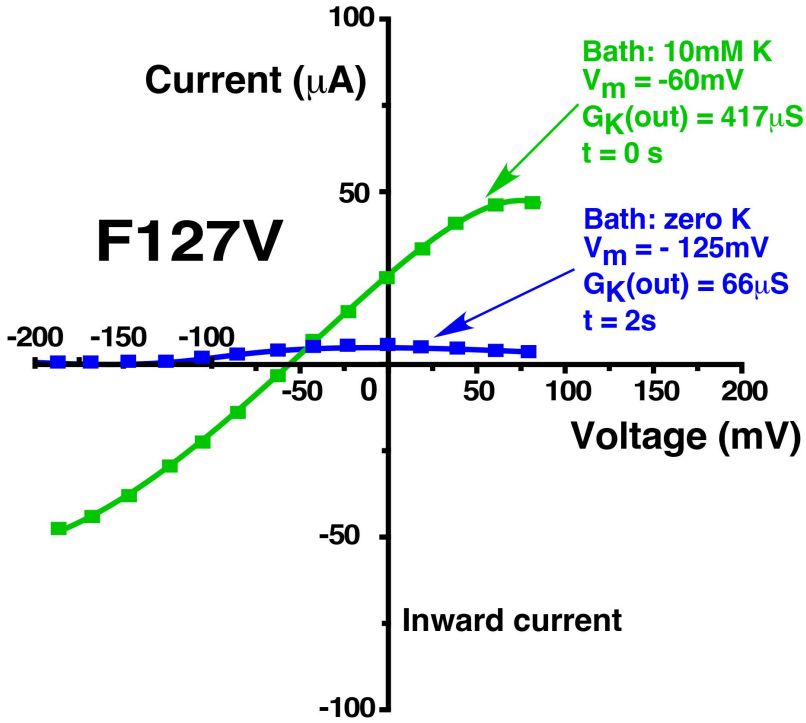

Figure 9. Representative example of a rapid decrease in F127V whole-cell outward conductance following replacement of 10 mM bath K with a zero K solution plus 15 mM 18-Crown ether (a K chelator) in Ca free conditions. Note the shift in reversal potential upon switching the bath from 10 mM K (−60 mV) to nominally zero K (−125 mV), assuming an oocyte internal [K] = 100 mM, as in previous protocols.

from 10 mM K to zero K produced a much slower decline in conductance (half time of 2 min) compared to F127V (half time of 0.1 min) and resulted in a final steady state conductance that was 3 times larger than what occurred with F127V (Figure 10).

This suggests that the F127V mutation allows a more rapid depletion of K from an unstirred layer adjacent to the outer mouth of the channel, thereby facilitating a faster decrease in conductance. The outward macroscopic conductances in Figure 10 were calculated as the slope of the I-V relation near the reversal potential, which varied between −60 mV at 10 mM K and −110 mV at zero bath K. Figure 10 does not apply to conductances in the voltage range (>80 mV) where F127V current was suppressed.

External Ca alters conductance and kinetics of F127V-Kir1.1b

In cell-attached patches on 5 oocytes, depolarized to zero membrane potential by 100 mM bath K, F127V single-channel conductance averaged 27 ± 1 pS with 100 mM K and zero Ca in the patch pipette (red line, Figure 11a). This is comparable to the 30 pS average F127V single-channel conductance reported in Figure 5 for a pipette K of 100 mM (zero Ca), but is substantially less than the 46.7 ± 2 pS conductance of wt-Kir1.1b with 100 mM external K and zero Ca (Figure 5) and ref [7].

Addition of 2 mM Ca to the 100 mM K pipette solution decreased F127V inward single-channel conductance from 27 ± 1pS (zero Ca) to 19 ± 2pS (2 mM Ca), a reduction of 30% (Figure 11a). This effect of external (pipette) Ca on inward single-channel conductance was qualitatively similar to what has been reported for voltage-dependent open-channel Ca block of Kir1.1b inward single-channel currents in excised patches with 10 mM K in the pipette [12]. Inward cell-attached channel currents were also recorded with 10 mM K in the patch pipette (external K) with and without 2 mM Ca in the pipette (external solution). Outward currents could not be unambiguously identified in F127V with 10 mM pipette K and were not included in the figure. Nonetheless, 2 mM Ca decreased channel inward conductance from 13

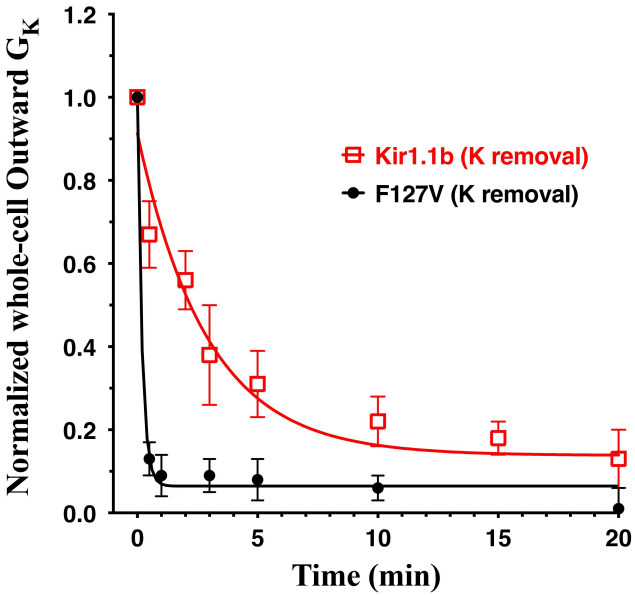

Figure 10. Decrease in whole-cell outward conductance (G_K) following transitions from 10 mM K to zero K plus 15 mM of the K chelator: 18-Crown-6 (catalog no. 274984, Sigma-Aldrich), in zero Ca solutions. Outward conductances were normalized to the initial conductance in 10 mM K. Data from F127V oocytes (n = 5) and wt-Kir1.1b oocytes (n = 6) were fitted to a first order exponential decay yielding half-times of 0.1 min for F127V and 2 min for Kir1.1b. Outward macroscopic conductances were calculated as the slope of the I-V relation near the reversal potential which varied between −60 mV at 10 mM K to −110 mV at zero bath K.

± 1pS (n = 4) to 10 ± 1pS (n = 4), a reduction of 23% (Figure 11b).

Single-channel F127V inward currents, representative of Figure 11a, were clearly visible with 100 mM K and 2 mM Ca in the patch pipette (Figure 12a). At a patch potential (V_{pch}) of −100 mV (in-out), the F127V open time of 17.9 ms with 2 mM Ca (Figure 12a,b) was not significantly different from the F127V open time of 19.4 ms without Ca (Figure 4b).

In contrast, F127V closed times were significantly affected by external Ca. The addition of 2 mM Ca to the 100 mM K pipette solution produced both a short closed time of 2.6 ms and a long closed time of 154 ms at V_{pch}= −100 mV (Figure 12b). This differs from the zero Ca condition where F127V displayed only a single closed time of 3.3 ms (Figure 4b). The Ca-induced long closed time of 154 ms significantly contributed to the decrease in F127V open probability from P_o = 0.86 (zero Ca, Figure 4b) to P_o = 0.76 (2 mM Ca, Figure 12b), at V_{pch}= −100 mV.

Although F127V inward single-channel currents were readily recorded with Ca in the pipette (Figure 12a), outward F127V single channel events were too small to be accurately resolved in the presence of external Ca at large positive voltages. This was not the case for wt-Kir1.1b, where both inward and outward channel currents could be unambiguously recorded with Ca in the pipette [13].

We also compared F127V kinetics to Kir1.1b kinetics in cell-attached patches on K-depolarized oocytes. With 100 mM K and 2 mM Ca in the pipette, the F127V open time of 17.9 ms (Figure 12b) was similar to the wt-Kir1.1b open time of 19 ms in cell-attached patches on K-depolarized oocytes [13]. On the other hand, the F127V closed times of 2.6 ms and 154 ms were both longer than the average wt-Kir1.1b closed times of 1.2 ms and 47 ms that have been previously reported for wt-Kir1.1b [13]. In addition, the F127V open probability of Po = 0.76 (Figure 12a,b) was significantly lower than the wt-Kir1.1b open probability of Po = 0.92, obtained with a similar patch potential of −100 mV [13]. This suggests that the mutation F127V affects channel gating by introducing an additional 154 ms long closed time into the Kir1.1 kinetics (Figure 12b).

External Ca suppresses F127V whole-cell current

External Ca also reduced whole cell inward and outward conductance much more with F127V than with wt-Kir1.1b (Figures 13,14). Addition of 5 mM external Ca to F127V oocytes bathed in 10 mM K decreased whole-cell conductance by 92% and depressed the large hump of outward current seen at positive membrane voltages, between 50 and 100 mV (Figure 13). In contrast, Ca produced only a modest (14%) decrease in wt-Kir1.1b whole-cell conductance (Figure 14), consistent with voltage dependent open channel block as previously reported [12].

Figures 13 and 14 depict the results of Ca elevation on either a single F127V or a single Kir1.1b oocyte. This allowed each oocyte to effectively function as its own control. Smooth curves drawn through the data of Figs 13 & 14 have no intrinsic meaning. Other F127V oocytes (n = 4) and Kir1.1b oocytes (n = 5), examined on different days, showed similar Ca dependence, but at

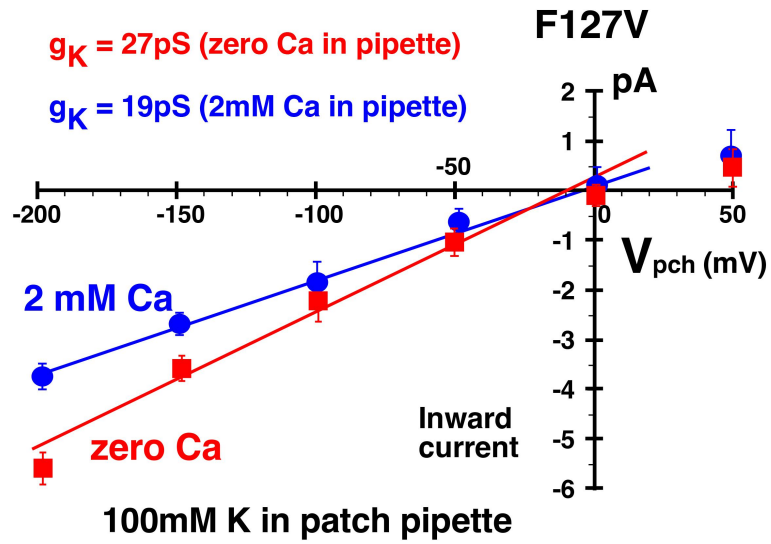

Figure 11a. Addition of 2 mM Ca decreased F127V inward single channel conductance from 27 ± 1pS (zero Ca, red line, n = 5 patches) to 19 ± 2pS (2 mM Ca, blue line) in 4 cell-attached F127V patches with 100 mM K in the pipette. Oocytes, with presumed 100 mM internal K, were depolarized to zero potential by 100 mM K in the bath. Hence the membrane patch potential, Vpch (in-out), equals the negative of the pipette command potential. Outward currents with Ca in the pipette were too small to be reliably resolved at positive potentials and were excluded from the linear fit.

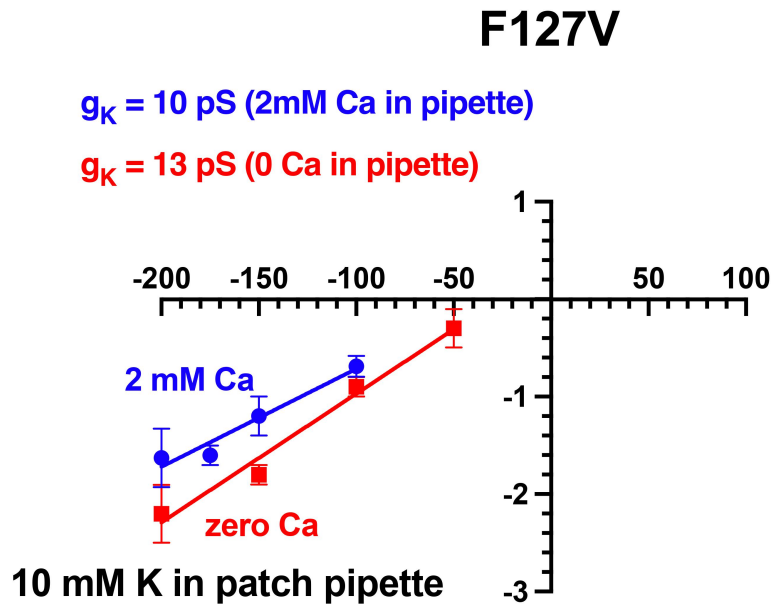

Figure 11b. Addition of 2 mM Ca decreased F127V inward single channel conductance from 13pS (zero Ca, red line) to 10pS (blue line) in cell-attached F127V patches with 10 mM K in the pipette. Oocytes, with presumed 100 mM internal K, were depolarized to zero potential by 100 mM K in the bath. Hence the membrane patch potential, Vpch (in-out), equals the negative of the pipette command potential. Outward currents with Ca in the pipette were too small to be reliably resolved at positive potentials and were excluded from the figure.

different absolute current levels. A pHo = 8.4 permeant acetate buffer was used to control the oocyte inside pH > 7.4 which guaranteed an open bundle crossing gate. The reversal potential of −59 mV for a 10:1 K ratio is consistent with the F127V oocytes having a high K selectivity.

The Ca-induced reduction in F127V macroscopic conductance (92%, Figure 13) was much larger than the Ca-induced reduction in single-channel conductance of 30% for 100 mM pipette K (Figure 11a) or 23% for 10 mM pipette K (Figure 11b). Since macroscopic current is a function of single-channel conductance, channel number, and open probability, this discrepancy between whole-cell and single-channel conductance implies that external Ca is affecting the gating (P_o) of F127V, but not the gating of wt-Kir1.1b, where Ca decreased whole-cell conductance by only 14% (Figure 14) and single-channel conductance by only 20% [12].

Discussion

Although permeation through K channels has been extensively investigated by crystallography and cryo-EM, details about the movement of K ions between selectivity filter and the outer solution remain somewhat murky. Early studies from MacKinnon's lab suggested that K enters and exits the selectivity filter from a partially hydrated (S_0) state [14], which is reached from an external fully hydrated (S_{ext}) state [5]

This K transition zone, adjacent to the outer mouth of the channel, has been particularly difficult to study in Kir1.1 inward rectifiers because a precise atomic structure for this channel is lacking. On the other hand, mutagenesis of residues near the outside of Kir1.1 may nonetheless provide information about K movement between selectivity filter and extracellular solution.

Our hypothesis is that an aromatic *Phe* at 127-Kir1.1b on each of 4 identical subunits increases the avidity of the channel for hydrated extracellular K ions (S_{ext}), which facilitates their transition to the partially hydrated S_0 state prior to entering the selectivity filter, where they could occupy any of the S_1-S_4 sites (Figure 15). Aromatic *Tyr* residues at a comparable location on Kir3.1, Kir 3.2, and Kir5.1 might function in a similar manner.

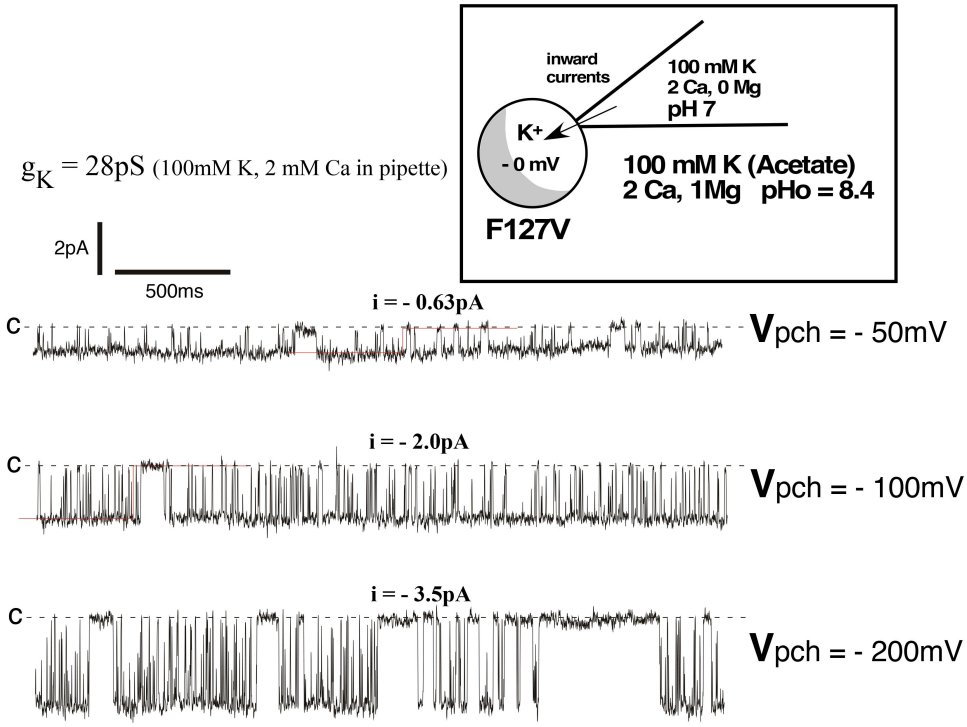

Figure 12a. Representative inward single-channel F127V currents from a cell-attached recording with 100mM K and 2 mM Ca in the pipette. Oocyte membrane potential was depolarized to near 0 mV by 100 mM K in the bath, causing Vpch(in-out) to equal the negative of the pipette command potential. Acetate buffer in bath solution set outside pH at 8.4 which stabilizes pHi at 7.4, causing a fully open bundle crossing gate. Downward deflections from the dashed closed line (c) denote inward K currents. At a patch potential (Vpch) of –100mV, open probability (Po) = 0.76.

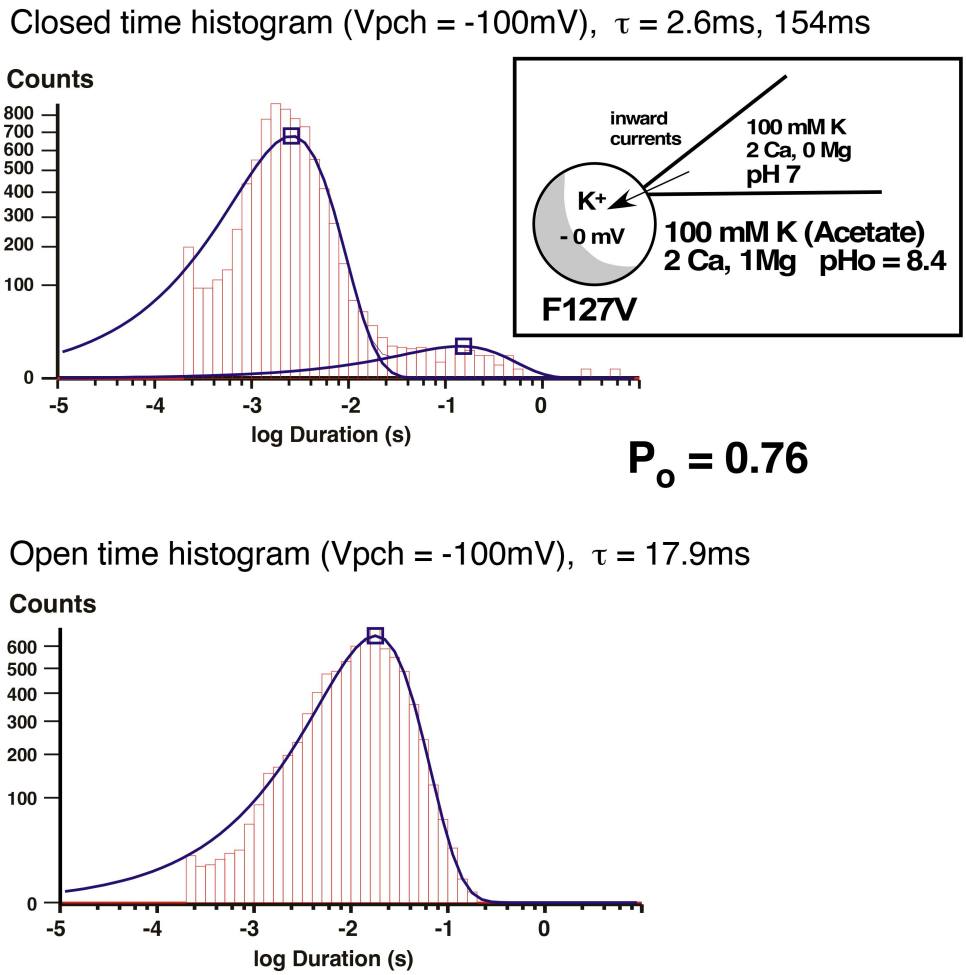

Figure 12b. Inward single-channel F127V currents in a cell-attached recording with 100mM K and 2 mM Ca in the pipette. Single channel inward conductance was 28pS. At Vpch = –100mV there was a single open time of 17.9ms and 2 closed times of 2.6ms and 154ms, resulting in a Po of 0.76.

We tested this hypothesis by replacing the *Phe* at 127-Kir1.1b with a small aliphatic *Val* and examined its effect on both single-channel and whole-cell conductance. Of particular interest was the impact of F127V-Kir1.1b on macroscopic outward K currents. Our results indicate that removal of the *Phe* at 127 suppresses outward currents that normally contribute to K secretion in the CCT and K recycling in the TALH (Figures 3,6). This voltage-dependent suppression of outward current could result from F127V destabilizing K adjacent to the outer mouth of the channel and altering its distribution in the selectivity filter, similar to what has been reported for KcsA under low K conditions [14].

Although we favor the idea that the F127V mutation reduces conductance by destabilizing K at the outer mouth of the channel, there may also be other interpretations. The increased rectification of F127V (Figure 3) compared to wt-Kir1.1b (Figure 2b) and the decrease in outward F127V macroscopic current (Figure 6) could be explained if F127V enhanced internal polyamine binding. However, the F127 residue is not one of the conserved pore-lining residues believed to interact strongly with polyamines [10,15]. Nonetheless, it's possible that the point mutation F127V-Kir1.1b allosterically alters polyamine binding in the permeation path to strengthen the degree of Kir1.1 inward rectification.

Comparison of Figures 7 and 8 suggest fundamental differences between polyamine block in the F127V mutant compared to wt-Kir1.1b. Decreases in external K produce a much greater decline in

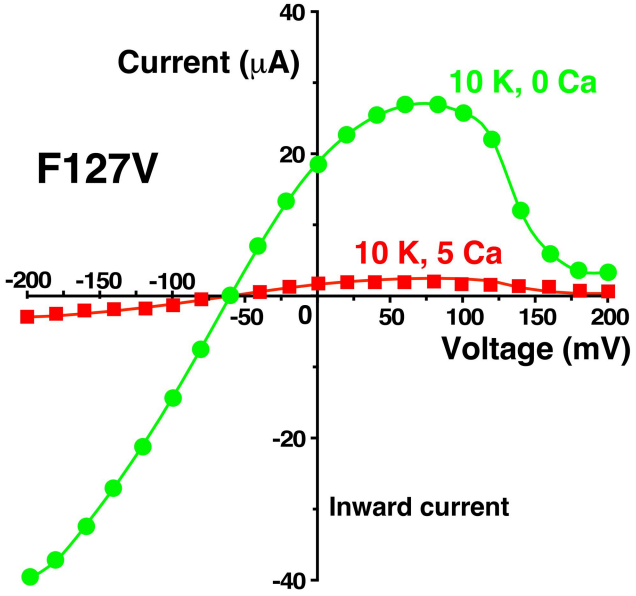

Figure 13. External Ca (5 mM) decreased F127V whole cell current and conductance to near zero in two-electrode voltage clamp experiments. Representative whole-cell current-voltage curves were obtained from an individual oocyte bathed in 10 mM K, zero Ca bath (green circles) followed by 10 mM external K and 5 mM Ca (red squares). Other oocytes ($n = 4$, obtained on different days) showed similar Ca dependence, but at different absolute current levels. Abscissa is oocyte membrane potential relative to bath (ground).

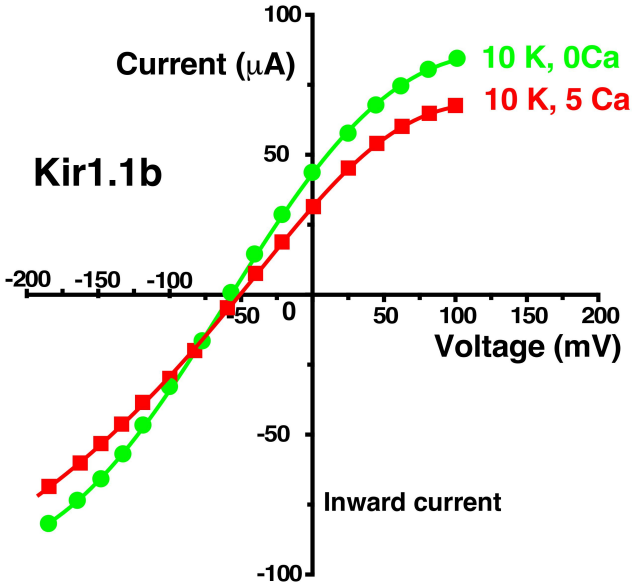

Figure 14. External Ca (5 mM) produced only a small decrease in wt-Kir1.1b whole cell current and conductance in two-electrode voltage clamp experiments. Representative whole-cell current-voltage curves were obtained from an individual oocyte bathed in 10 mM K, zero Ca bath (green circles) followed by 10 mM external K and 5 mM Ca (red squares). Other oocytes ($n = 5$, obtained on different days) showed similar Ca dependence, but at different absolute current levels.

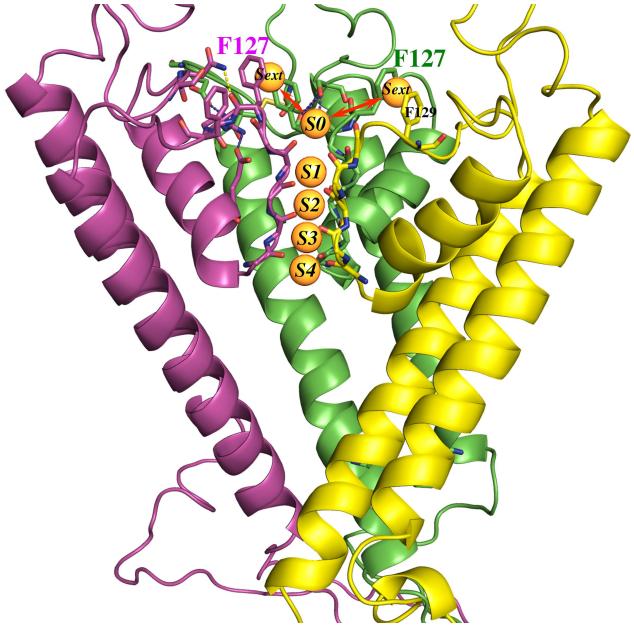

Figure 15. Homology model of Kir1.1b in the closed state, showing 3(of 4) identical subunits (each in a different color). Aromatic residues F127 and F129 from each subunit are at the extracellular end of the permeation path. Five specific K binding sites (S0 to S4) are located along the Kir1.1b permeation path. The K ions at S0 and S4 are presumably half hydrated, and the K ions at S_{ext} are probably fully hydrated. Model generated using MOE (Molecular operating environment, Montreal, Canada) with the closed-state 3.1 angstrom crystal structure of the chicken inward rectifier Kir2.2 (3JYC) as template.

F127V inward and outward current (Figure 8), relative to wt-Kir1.1b (Figure 7), which implies that F127V can be easily depleted of conductive K ions by a reduction of external K. Furthermore F127V exhibits almost a complete suppression of outward current at large positive voltages (Figure 8), which suggests that K can be electrostatically driven away from the outer mouth of the channel by a sufficiently positive potential.

Further support for the hypothesis that the F127V mutant decreases the avidity of the channel for external K comes from the K-dependence of F127V and wt-Kir1.1b single channel conductances (Figure 5). In paired experiments F127V had a significantly lower K affinity ($K_m = 33 \pm 4$ mM) than wt-Kir1.1b ($K_m = 7.7 \pm 1$ mM). This supports the idea that the absence of *Phe* at 127 weakens the channel's interaction with external K ions, allowing positive voltage to disperse K ions away from the outer mouth of the channel, causing reduced outward K current and conductance in the F127V mutant.

Additional evidence that the F127V mutation destabilizes external K ions comes from a comparison of the decrease in F127V and wt-Kir1.1b conductance during complete removal of external K in 2 sec, using the K chelator 18-Crown-6. In these experiments, the normalized F127V half time was 6 sec, compared to 2 min for wt-Kir1.1b (Figure 10). This is consistent with the outer mouth of F127V being less hospitable than wt-Kir1.1b to external K.

Finally, our results with Ca support the idea that external Ca acts synergistically with voltage to destabilize K near F127V at the S_{ext} site (Figure 15), possibly altering the K distribution in the filter, and gating the channel closed. This could occur, in addition to Ca producing a modest open-channel block of inward current. Evidence for gating of F127V by external Ca comes from a comparison of Ca-induced decreases in macroscopic vs single-channel conductances. Addition of Ca to the external solution decreased whole cell macroscopic conductance by 92% (Figure 13), but reduced F127V single-channel conductance by only 30% with 100 mM K in the pipette (Figure 11a) and by 23% with 10 mM K in the pipette (Figure 11b).

In either case, the discrepancy between reductions in macroscopic vs single channel conductance imply that external Ca is decreasing either F127V open probability or channel number. If we assume no change in channel number, this would be consistent with external Ca gating F127V by decreasing open probability. Additional support for Ca gating of F127V comes from the induction of a 154 ms F127V long closed time by external Ca. Importantly, there was no evidence of external Ca gating wt-Kir1.1b since Ca produced only a modest 14% block of macroscopic (whole-cell) conductance (Figure 14) compared to a 20% block of single-channel conductance [12]. Consequently, the decrease in wt-Kir1.1b macroscopic current can be largely explained by open channel Ca block of channel conductance, without a change in open probability.

It's not exactly clear how external Ca interacts with F127V to affect channel gating. One possibility is that Ca displaces K ions that would normally interact with F127 at the S_{ext} locus and disrupts their transition to the partially hydrated S_0 locus (Figure 15). If so, this would affect the distribution of K in the selectivity filter, causing a decrease in macroscopic F127V current and conductance. This would be consistent with our hypothesis that normally the *Phe* residue at 127-wt-Kir1.1b stabilizes outer K ions at the external S_{ext} site. We speculate that this could be a consequence of the aromatic *Phe* forming a cation-Pi interaction with the outer K ions at S_{ext}, which would allow better access of K to the S_0 site, facilitating K entry and exit to and from the filter (Figure 15). Additional aromatics at F129-Kir1.1b and *Tyr* residues in comparable locations on Kir3.1 and Kir4.1 may also be involved in cation-Pi interactions as well.

In conclusion, we've provided support for the hypothesis that an aromatic *Phe* at the outer mouth of wt-Kir1.1b allows outward K current over a wide range of membrane potentials and Ca concentrations, consistent with physiological K secretion in this weak inward rectifier. Our evidence comes from the suppression of both single-channel and macroscopic outward current following replacement of this aromatic *Phe* with a small aliphatic *Val*. Although the resulting reduction of outward current resembles strong inward rectification, our observations cannot be explained by polyamine block alone, but could be explained by voltage driven depletion of K ions from the outer mouth of the channel (Figure 15).

Furthermore, affinity comparisons between the F127V mutant and wt-Kir1.1 during progressive elevation of external K imply that the *Phe* residue at 127-Kir1.1b enhances the avidity of the channel for extracellular K near the outer mouth of the channel (at the S_{ext} site). In addition, the *Phe* residue appears to slow K depletion adjacent to the outside of the channel during complete removal of K from the external solution. Finally, voltage-dependent suppression of F127V outward current by external Ca supports our hypothesis that the *Phe* at 127-Kir1.1b is critical for facilitating secretory K current in the renal CCT and TALH under physiological conditions.

Acknowledgments

I would like to thank Lawrence G. Palmer, Prof at Weill-Cornell Medical College, for helpful discussions and critical reading of the manuscript.

Disclosure statement

No potential conflict of interest was reported by the author(s).

Funding

The author(s) reported there is no funding associated with the work featured in this article.

Data availability statement

The data that support the findings of this study are available from the corresponding author, [HS], upon reasonable request.

ORCID

Henry Sackin http://orcid.org/0000-0002-2886-9213

References

[1] Hansen SB, Tao X, MacKinnon R. Structural basis of PIP2 activation of the classical inward rectifier K+ channel Kir2.2. Nature. 2011 Aug 28;477 (7365):495–498. doi: 10.1038/nature10370

[2] Tao X, Avalos JL, Chen J, et al. Crystal structure of the eukaryotic strong inward-rectifier K+ channel Kir2.2 at 3.1 a resolution. Science. 2009 Dec 18;326 (5960):1668–74. doi: 10.1126/science.1180310

[3] Whorton MR, MacKinnon R. Crystal structure of the mammalian GIRK2 K+ channel and gating regulation by G proteins, PIP2, and sodium. Cell. 2011 Sep 30;147 (1):199–208. doi: 10.1016/j.cell.2011.07.046

[4] Martin GM, Yoshioka C, Rex EA, et al. Cryo-EM structure of the ATP-sensitive potassium channel illuminates mechanisms of assembly and gating. Elife. 2017 Jan 16;6:e24149.

[5] Bernèche S, Roux B. Energetics of ion conduction through the K+ channel. Nature. 2001 Nov 1;414 (6859):73–77. doi: 10.1038/35102067

[6] Choe H, Zhou H, Palmer LG, et al. A conserved cytoplasmic region of ROMK modulates pH sensitivity, conductance and gating. Am J Physiol. 1997;273(4):F516–F529. doi: 10.1152/ajprenal.1997.273.4.F516

[7] Sackin H, Nanazashvili M, Palmer LG, et al. Structural locus of the pH gate in the Kir1.1 inward rectifier channel. Biophys J. 2005 Apr;88(4):2597–2606.

[8] Lopatin AN, Nichols CG. [K^+] dependence of polyamine-induced rectification in inward rectifier potassium channels (IRK1, Kir2.1). J Gen Physiol. 1996 Aug;108(2):105–113. doi: 10.1085/jgp.108.2.105

[9] Murata Y, Fujiwara Y, Kubo Y. Identifcation of a site involved in the block by extracellular Mg^{2+} and Ba^{2+} as well as permeation of K^+ in the Kir2.1 K^+ channel. J Physiol (Cambridge). 2002;544(3):665–677. doi: 10.1113/jphysiol.2002.030650

[10] Kurata HT, Phillips LR, Rose T, et al. Molecular basis of inward rectification: polyamine interaction sites located by combined channel and ligand mutagenesis. J Gen Physiol. 2004 Nov;124(5):541–554.

[11] Nichols CG, Lopatin AN. Inward rectifier potassium channels. Annu Rev Physiol. 1997;59(1):171–191. doi: 10.1146/annurev.physiol.59.1.171

[12] Yang L, Edvinsson J, Sackin H, et al. Ion selectivity and current saturation in inward-rectifier K+ channels. J Gen Physiol. 2012;139(2):145–157. doi: 10.1085/jgp.201110727

[13] Chepilko S, Zhou H, Sackin H, et al. Permeation and gating properties of a cloned renal K^+ channel. Am J Physiol. 1995;268(2):C389–C401. doi: 10.1152/ajpcell.1995.268.2.C389

[14] Zhou Y, Morais-Cabral JH, Kaufman A, et al. Chemistry of ion coordination and hydration revealed by a K+ channel–fab complex at 2.0 Å resolution. Nature. 2001;414(6859):43–48. doi: 10.1038/35102009

[15] Nichols CG, Lee SJ. Polyamines and potassium channels: a 25-year romance. J Biol Chem. 2018 Nov 30;293 (48):18779–18788. doi: 10.1074/jbc.TM118.003344